

All solid-state comb-like network polymer electrolytes based on poly(methylsiloxane)

Hui Jiang, Shibi Fang*

Institute of Chemistry, Chinese Academy of Sciences, Beijing 100080, PR China

Received 19 August 2005; received in revised form 2 November 2005; accepted 4 November 2005

Available online 20 December 2005

Abstract

All solid-state comb-like network polymer electrolytes (CNPE) based on poly(methylsiloxane) with pendant PEO chains as internal plasticizing chains (IPC) have been designed and synthesized. Ultraviolet (UV) polymerization method was applied for the curing of CNPEs. Effects of the network structure on the conductive properties and mechanical properties were discussed in details. Ionic conductivity of the prepared CNPE is one order of magnitude larger than those without IPCs, which suggests that the expected drop of conductivity caused by crosslinking has been well compensated by the introduction of IPCs. Maximum conductivity of $1.01 \times 10^{-4} \text{ S cm}^{-1}$ and maximum tensile strength of 0.66 MPa were obtained at 30 °C. Electrochemical stability and electrolyte/electrodes interfacial stability properties were evaluated by cyclic voltammetry and ac impedance, respectively.

© 2005 Elsevier B.V. All rights reserved.

Keywords: All solid-state; Comb-like polymer electrolyte; Ionic conductivity; Mechanical property; UV polymerization

1. Introduction

Recently, electric vehicles (EV) and engine/battery hybrid vehicles (HEV) have become the subject of active research and development, in order to abate both the energy crisis and environmental pollution. A lithium battery using all solid-state polymer electrolytes can provide the energy source for EV/HEV. All solid-state polymer electrolytes make the fabrication of safe and reliable batteries possible, and allow development of thin, flexible and/or irregular shape batteries. Furthermore, all solid-state polymer electrolytes can increase the energy density to achieve high performance lithium battery, which play the role of separator in lithium battery. Among the polymer electrolytes reported, poly(ethylene oxide)–lithium salt (PEO–LiX) complexes have been investigated the most widely, because they are more stable and have higher ionic conductivity than those containing any other group of solvating polymers [1–4]. However, the ionic conductivity of PEO–LiX electrolyte remains very low ($\leq 10^{-6} \text{ S cm}^{-1}$) at room temperature due to the crystalline nature of PEO. Only at high temperatures can it reach practi-

cal value ($\geq 10^{-4} \text{ S cm}^{-1}$). Also, most of today's commercial lithium batteries are based on gel polymer electrolytes (GPE), which are widely applied in portable electronic devices. Yet, lithium batteries based on GPEs are not so qualified for EV and HEV, for their inherent drawbacks, such as poor mechanical properties, bad electrochemical stability of interfaces with electrodes [5–7].

The comb-like polymer electrolytes have been found to be attractive for all solid-state lithium battery [8–12]. Comb-like polymers, often containing oligomeric PEO as side chains, and polar subunits, such as acrylonitrile, methacrylic acid, boric acid and acrylamide, were arranged along the chains to promote dissociation of lithium salt. Such polymers provide pendant ion-coordinating ether side chains with high ionic conductivity, because the fast ionic transport and fast side chain motion will increase the mobility of the dissolved ions. The maximum conductivity at ambient temperature of the reported comb-like polymer electrolytes is around $10^{-5} \text{ S cm}^{-1}$ [13–15], which is an order of magnitude less than the required conductivity for lithium batteries ($\geq 10^{-4} \text{ S cm}^{-1}$). Besides, the mechanical properties of these systems do not allow the systems be used as separator for lithium battery due to the presence of flexible amorphous phase.

* Corresponding author. Tel.: +86 10 62613252; fax: +86 10 62559373.
E-mail address: fangsb@iccas.ac.cn (S. Fang).

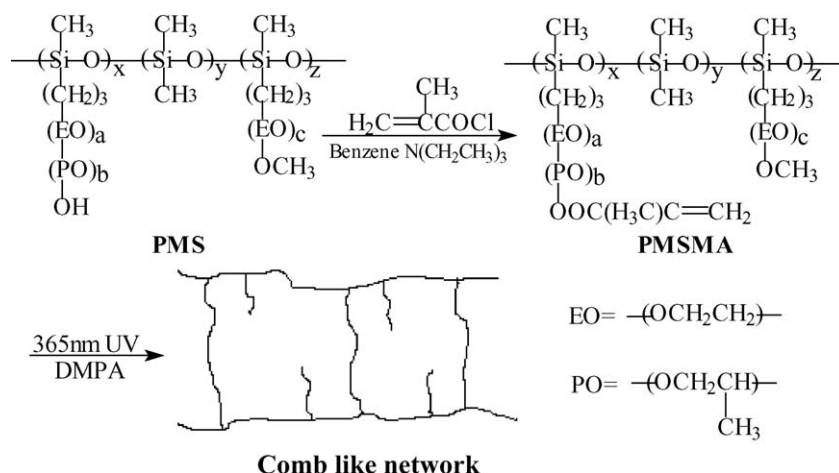


Fig. 1. Preparation schemes of comb-like network polymer electrolyte (CNPE).

In the present study, we report a new and effective approach to improve the balanced characteristics of conductivity, mechanical properties and interfacial stability of all solid-state polymer electrolytes. As shown in Fig. 1, a comb-like network polymer has been designed and synthesized. Highly flexible poly(methylsiloxane) backbones allow a high chain mobility. The possible crystallization of PEO side chain is suppressed by block polymerization with propylene oxide (PO). Short PEO chains were introduced to the backbones as internal plasticizing chain (IPC) in order to enhance the conductivity. The network structure of polymer matrix imparts electrolyte film excellent mechanical properties. Ultraviolet (UV) were utilized for the curing of the prepolymer, which proves to be a quicker, low energy consumed and high efficiency method in comparison with the traditional thermal curing one.

2. Experimental

2.1. Materials and pretreatment

Poly(hydromethyl siloxane) (PHMS), poly(ethylene glycol)-methyl ether (PEGME) ($M_n = 350, 550, 750$), 2,2-dimethoxy-2-phenylacetophenone (DMPA) were purchased from Aldrich. Lithium perchlorate (LiClO_4) (Acros) dried in vacuum under 140°C for 48 h before use. Allyl chloride, α -methacryloyl chloride (Haimen Best Fine Chemical Co. Ltd.) used after freshly distilled under reduced pressure. Allyl terminated poly(ethylene oxide-propylene oxide) copolymer (PEO-PPOH) ($M_n = 1096, 1180, 1264, 2120, 2302, 2484$) were supplied by Nanjing Plastic Factory. PHMS, PEGME and PEO-PPOH were dehydrated over molecular sieves (4 \AA) for 7 days before use.

2.2. Preparation of all solid-state comb-like network polymer electrolytes

Preparation scheme of all solid-state comb-like network polymer electrolytes is shown in Fig. 1. A sealed bottle with 0.1 mol of modified poly(methylsiloxane) (PMS) and $0.15x$ mol of triethylamine (dissolved in benzene beforehand) were placed in

an ice-water bath. Then $0.15x$ mol of α -methacryloyl chloride were titrated very slowly to the bottle under vigorous stirring. The reaction was continued at 30°C for 24 h after titration finished. Triethylamine hydrochloride and excessive α -methacryloyl chloride were washed off by water several times. The remained solution was evaporated under reduced pressure after being dried over MgSO_4 . The resultant product, PMSMA was dehydrated over molecular sieves (4 \AA). Accurate amounts of DMPA, LiClO_4 and tetrahydrofuran (THF) were added to prepolymer (PMSMA), then forming a transparent solution by vigorous stirring. The solution was evaporated under reduced pressure until no THF remains. The obtained viscous liquid mass was then cast onto a flat square Teflon mold. Then the mold was exposed to UV (365 nm , 10 mW cm^{-2}) for 10 min, subsequently a light yellow, transparent and elastic film was obtained. Before any measurement, the film is dehydrated in a vacuum oven at 80°C for 24 h. All electrochemical measurements were performed under dry argon atmosphere. The synthesis of PMS is according to our previous work [16]. As shown in Fig. 1, the structures of the backbone and the side chain of PMS can be adjusted by regulating the six parameters: x, y, z, a, b and c .

2.3. Measurements

The conductivity of electrolytes (σ) was measured by using HIOKI LCR 3520 Hi TESTER at 1 kHz. The experimental procedure was the following: a disk of diameter (D) is cut from the electrolyte film. It is placed in the center hole of a Teflon spacer ring and compressed by two stainless steel (SS) rod at the opposite ends of the spacer ring. The thickness of samples (T) was taken to be the Teflon spacer thickness. The conductivities were calculated by the formula below:

$$\sigma = \frac{4T}{\pi R D^2} \quad (R \text{ is the measured resistance of sample}). \quad (1)$$

Stress-strain measurements were performed to characterize the mechanical properties of the CNPE. The tensile strength and elongation at break were measured by an autograph (Minimat-2000, Pheometric Scientific Inc., USA) with a constant elonga-

tion rate of 50 mm min^{-1} . All the stress–strain measurements were performed at 30°C with a relative humidity of 30%.

Cyclic voltammetry of CNPEs is measured by using a Solartron potentiostat Model S1 1287 electrochemical interface to evaluate electrochemical stability. The film samples were assembled into a Li/CNPE/SS cell in the same way as in conductivity measurement. Metallic Li was used as counter and reference electrodes, and SS as the working electrode. Scanning rate of sample film is 5 mV s^{-1} .

The Li/electrode interface stability was studied by ac impedance spectroscopy, using an EG&PAR potentiostat coupled with a Solartron Model 1260 frequency response analyzer. The 10 mV ac amplitude was applied with frequency sweeping from 0.1 Hz to 1 MHz . A symmetric cell structure, Li/CNPE/Li, was utilized in the measurement.

3. Results and discussion

3.1. Characterization of comb-like network polymer electrolyte (CNPE)

Figs. 2 and 3 are FT-IR spectra of PMS and PMSMA. There are almost the same except that: (1) the $-\text{OH}$ (3482 cm^{-1}) peak in Fig. 2 is completely disappeared in Fig. 3; (2) the $-\text{COO}$ (1727 cm^{-1}) peak and the $\text{C}=\text{C}$ (804 cm^{-1}) sharp peak appear in Fig. 3, which indicates the complete conversion of PMS to PMSMA. FTIR spectra data are the following: 3482 cm^{-1} ($-\text{OH}$), $2968\text{--}2869 \text{ cm}^{-1}$ ($-\text{CH}_3$), 1727 cm^{-1} ($-\text{COO}$), 1455 cm^{-1} ($\text{C}-\text{H}$), 1373 cm^{-1} ($-\text{CH}_3$),

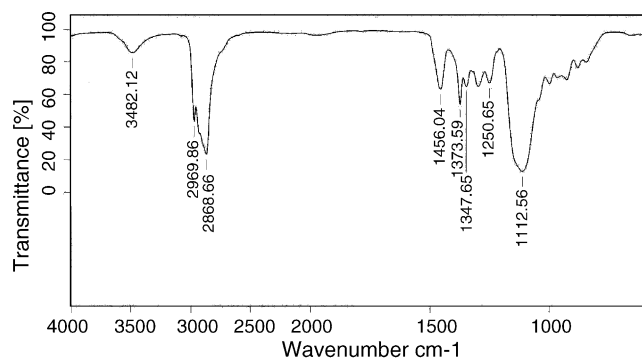


Fig. 2. FT-IR spectra of PMS.

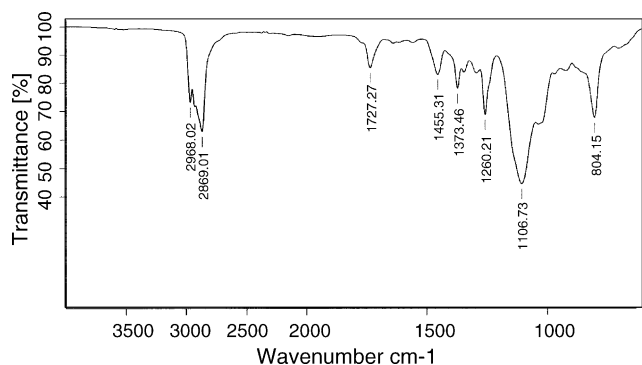


Fig. 3. FT-IR spectra of PMSMA.

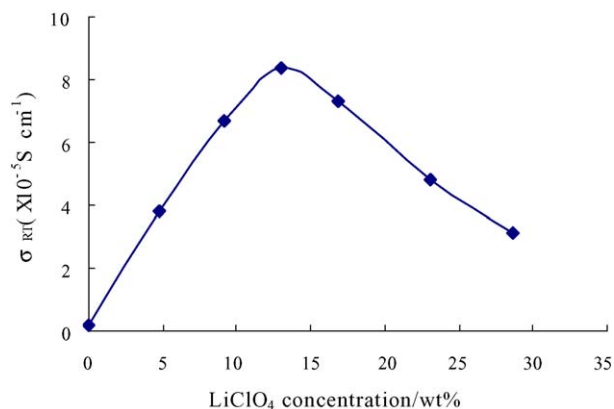


Fig. 4. Ionic conductivity as a function of LiClO_4 concentration (wt%) ($x=24$, $y=68$, $z=8$, $a=b=20$, $c=12$, $t=30^\circ\text{C}$).

$1250\text{--}1260 \text{ cm}^{-1}$ ($\text{Si}-\text{C}$), $1106\text{--}1112 \text{ cm}^{-1}$ ($\text{H}_2\text{C}-\text{O}-\text{CH}_2$), 804 cm^{-1} ($\text{C}=\text{C}$). The ^1H NMR (CDCl_3) data of PMSMA were the following: δ (ppm) 0.10 ($-\text{SiCH}_3$), 1.20 ($-\text{CH}_3$), 1.70 ($-\text{CH}_2\text{CH}_2\text{CH}_2-$), 3.35 ($-\text{OCH}_3$), 3.65 ($-\text{OCH}_2\text{CH}_2\text{O}-$). The absence of the peak of $-\text{OH}$ (4.30 ppm) further confirmed the structure of PMSMA. The conversion ratio of $-\text{OH}$ to methacryloyl groups was 0.98 as determined by ^{13}C NMR.

3.2. Ionic conductivity study

One of the most important challenges of all solid-state polymer electrolytes is to increase its room temperature ionic conductivity to the practical level ($\geq 10^{-4} \text{ S cm}^{-1}$). The conductivity of solid polymer electrolytes (SPEs) reads:

$$\sigma(T) = \sum n_i q_i \mu_i \quad (2)$$

where i indicates the kind of carrier, n is the density of carrier, q is the number of electric charge and μ is the mobility [17]. Series of ionic conductivity study on CNPEs were performed as follows. The effect of LiClO_4 concentration on the ionic conductivity of CNPE at room temperature is shown in Fig. 4. It can be seen that the maximum conductivity ($8.35 \times 10^{-5} \text{ S cm}^{-1}$) appeared at $[\text{EO}]/[\text{Li}^+] = 7.8/1$ (mol/mol) (13 wt% concentration of LiClO_4), which is slightly lower than the traditional theory value $[\text{EO}]/[\text{Li}^+] = 8/1$ (mol/mol), which can be considered as the PO segment partly taking the place of EO [18]. At low LiClO_4 concentration ($<13 \text{ wt}\%$), there are insufficient current carriers of Li^+ ions in the system, which lead to poor conductivity. Saturation of free Li^+ ions density appears of LiClO_4 concentration of 13 wt%. At high LiClO_4 concentration ($>13 \text{ wt}\%$), Li^+ ions begin to condense with each other. Given the big Li^+ ions mass, it is more difficult for Li^+ ions to move through the polymer matrix.

3.2.1. Effect of network structure on ionic conductivity

The backbone structure of CNPE was determined by three parameters: x , y and z . The x and z correspond to the numbers of the crosslinked side chains (CSC) and IPC, respectively. Table 1 illustrates the effect of poly(methylsiloxane) backbone structure on ionic conductivity. The ratio of x/z (crosslinked chain/internal

Table 1
Effect of poly(methylsiloxane) backbone structure on ionic conductivity

Sample ^a no.	Backbone structure parameters			Ionic conductivity (S cm ⁻¹)
	x	y	z	
1	6	92	2	6.14×10^{-5}
2	12	84	4	1.01×10^{-4}
3	24	68	8	8.35×10^{-5}
4	36	52	12	4.32×10^{-5}
5	39	48	13	3.37×10^{-5}

^a Other parameters of samples are the following: LiClO₄ = 13 wt%, $a = b = 20$, $c = 12$, $t = 30$ °C.

plasticizing chain) was fixed at 3/1. The conductivities range from 3.37×10^{-5} to 1.01×10^{-4} S cm⁻¹ in Table 1. It is evident that with the decrease of x , the conductivity increases. The maximum conductivity of 1.01×10^{-4} S cm⁻¹ appeared at $x = 12$, almost three times higher than that of $x = 39$. As it can be seen from the network scheme in Fig. 1, while the x increases higher crosslinking density obtained. The low conductivity is due to the high crosslinking density that hindered ionic transportation much. In addition, the free length of poly(methylsiloxane) backbone was relatively restricted by crosslinking points, leading to the low chain mobility. The increased conductivity was attributed to the short PEO internal plasticizing chains appended to the backbones, and the relatively high backbone mobility to the low crosslinking density. It is interesting to note that the sample 1 possesses the lowest crosslinking density in Table 1, but its conductivity is slightly reduced. It is well known that the PEO chain is the most efficient polymer in dissolving and ionizing LiClO₄, while the poly(methylsiloxane) backbone is not so effective. It is clear that the lower conductivity of sample 1 than that of sample 2 is due to the lower density of EO segment in CSC.

Fig. 5 shows the effects of the structure and the length of CSC to ionic conductivity. It can be seen that CNPE with pure PEO or pure poly(propylene oxide) (PPO) side chain remains relatively low conductivity. As noticed before, PEO is the most efficient polymer in dissolving and ionizing LiClO₄. However, long PEO chain tends to crystalline at room temperature, which hinders ionic transportation. And PPO chain is much inefficient in dissolving LiClO₄ and ions transport. That is why the con-

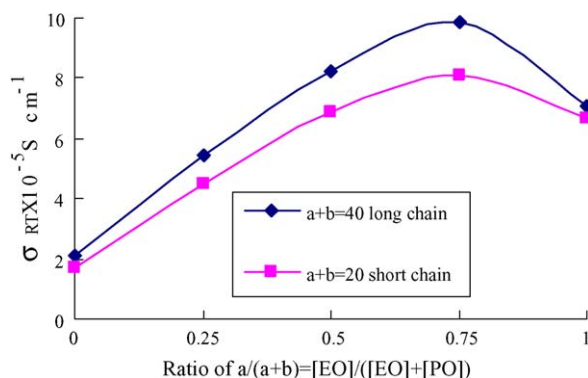


Fig. 5. Dependence of ionic conductivity on the relatively content of EO segment in CSCs ($x = 24$, $y = 68$, $z = 8$, $c = 12$, LiClO₄ = 13 wt%, $t = 30$ °C).

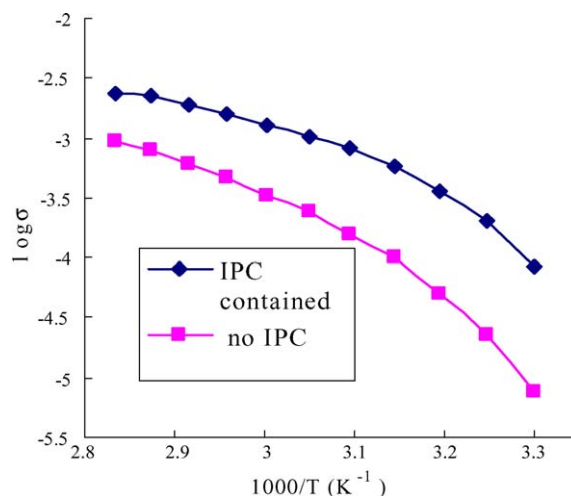


Fig. 6. Dependence of ionic conductivity for CNPEs with and without IPC on temperature ($x = 24$, $y = 68$, $z = 8$, $a = b = 20$, $c = 12$ or 0 (CNPE without IPC), LiClO₄ = 13 wt%).

ductivity of CNPE with pure PPO side chain is much lower than that of pure PEO. The ionic conductivity rises with the increase of CSC length and the relatively content of EO segment in CSC. However, the effect of CSC length is not so significant, which can be seen in Fig. 5. Longer side chain means larger size network lattice and higher chain mobility. The maximum conductivity 9.88×10^{-5} S cm⁻¹ is reached when the ratio of [EO]/([EO] + [PO]) approaches 0.75.

The temperature dependence of the ionic conductivity for CNPEs is shown in Fig. 6, with and without IPCs. It is obvious that the conductivities increase with the increasing of temperature. It is evident that the plots of $\log \sigma$ versus $1/T$ deviate from linear, which suggests that ion transport follows the Vogel–Tamman–Fulcher (VTF) equation [19–21], indicating that ion transport is correlated with the segmental motion of the polymer chain [22,23]. As noticed, the conductivity of IPC contained CNPE remains consistently higher than that of CNPE without IPC at all the temperature measured. Especially at ambient temperature the conductivity of the former is one magnitude higher than that of the latter. It is attributed to the short internal plasticizer PEO chains introduced to poly(methylsiloxane) backbones and relatively high backbone mobility.

3.3. Mechanical property

Table 2 shows the effect of poly(methylsiloxane) backbone structure on mechanical property of CNPE. The tensile strength is increased with the increase of x , while the elongation is decreased with the increase of x . The increase of x means to increase crosslinking points, thus resulting in high crosslinking density. Further increase of x will lead to poor conductivity because the film becomes more rigid with little flexibility. It is interesting to note that low value of x will cause the difficulty of curing, where only a viscous glue-water-like mass was obtained, which is not suitable as separator in lithium batteries. Table 3 shows the effect of side chain structure on mechanical property of CNPE. The tensile strength rises smoothly with

Table 2
Effect of poly(methylsiloxane) backbone structure on mechanical property

Sample ^a no.	<i>x</i>	<i>y</i>	<i>z</i>	<i>a</i>	<i>b</i>	<i>c</i>	Strength at break (MPa)	Elongation at break (%)
1	6	92	2	20	20	12	0.07	45
2	12	84	4	20	20	12	0.16	35
3	24	68	8	20	20	12	0.33	28
4	36	52	12	20	20	12	0.48	21
5	39	48	13	20	20	12	0.54	17

^a Other parameters of samples are the following: LiClO₄ = 13 wt%, ratio of CSC/IPC = *x/z* fixed on 3/1, 30 °C.

Table 3
Effect of side chain structure on mechanical property

Sample ^a no.	<i>x</i>	<i>y</i>	<i>z</i>	<i>a</i>	<i>b</i>	<i>c</i>	Strength at break (MPa)	Elongation at break (%)
1	24	68	8	0	40	12	0.25	32
2	24	68	8	10	30	12	0.28	30
3	24	68	8	20	20	12	0.33	28
4	24	68	8	30	10	12	0.38	25
5	24	68	8	40	0	12	0.49	22
6	24	68	8	10	10	12	0.66	13

^a Other parameters of samples are the following: LiClO₄ = 13 wt%, 30 °C.

the increase of *a* (the relative content of EO segment versus PO in CSC) from sample 1 to sample 5. Longer regular PEO chains has a tendency of crystallization, which increase the strength of polymer matrix, but it is difficult for PPO chains to be crystallization for it is not so regular. Sample 6 holds the maximum strength 0.66 MPa in all the sample measured, for it has higher crosslinking density attributed to short crosslinked side chains.

3.4. Electrochemical stability

The typical cyclic voltammetry (of sample 3 in Table 2) is shown in Fig. 7, which is obtained by sweeping sample film on a SS electrode in a Li/CNPE/SS structure cell, at a scanning rate of 5 mV s⁻¹. It suggests that the electrolyte exhibits excellent electrochemical stability till 4.3 V versus Li/Li⁺. The cathode peak at about -0.5 V in the first cycle corresponds to plating of lithium on SS electrode. The cathode peak is eliminated in the following cycles. There is hardly oxidation peak across all the scanned voltage range (-0.5 to +5.0 V). Thus, it implies that the lithium deposition/dissolution are almost completely reversible

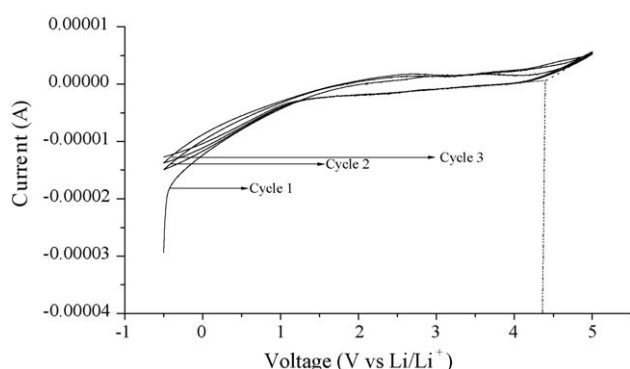


Fig. 7. Cyclic voltammetry curves of sample 3 in Table 2 in a Li/CNPE/SS cell (30 °C).

[24]. It seems that the sample does not decompose until 4.3 V versus Li/Li⁺.

3.5. Electrolyte/electrodes interfacial stability

Fig. 8 shows the time evolution of the impedance spectrum in a symmetric cell, Li/CNPE/Li, stored under open circuit condition at 25 °C. Impedance responses of CNPE are cole-like semicircle in high frequency. The intercept of the semicircle shaped curves with the horizontal-axis corresponds to the bulk resistance (*R_b*), and the value of the diameter of the semicircle is equal to the total resistance of both interfaces (*R_i*) [25]. The time evolution of the interface resistance *R_i* is shown in Fig. 8. The maximum value of *R_i* is at about 24 h. Then *R_i* decreases to some extent and becomes stabilized near the initial value for about more than 3 days. Thus, it demonstrates that the formation of passivation film at the interface between the CNPE and the lithium electrode is not severe, but almost reversible. Passivation film at the interface may be produced by the reac-

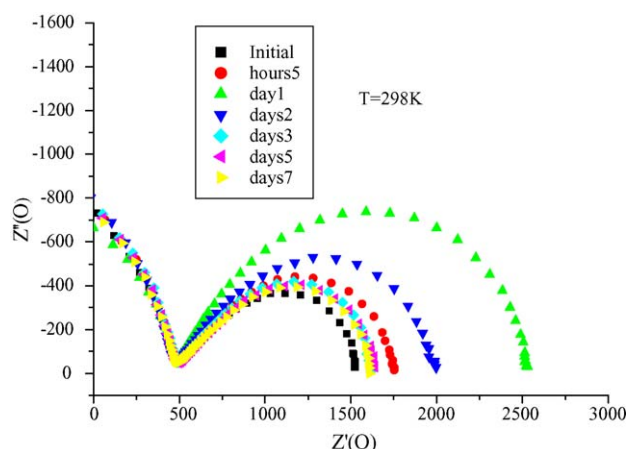


Fig. 8. The impedance spectra of sample 3 in Table 2 at 25 °C.

tion of the lithium electrode with CNPE. As the all solid-state electrolyte there should be no aprotic solvent, no water and no oxygen in the test cells, the reaction process can be reversible [26,27]. In another word, passivation film may reorganize itself spontaneously and becomes thinner and more uniform and more compact. The bulk resistance R_b is almost constant with the time, which implies that CNPEs does not decompose and has good dimensional stability under inner pressure.

4. Conclusion

All solid-state network polymer electrolytes based on poly(methylsiloxane) has been designed and synthesized. Short PEO chains were pended to the backbones as an IPC to enhance the conductivity. Ionic conductivity of CNPE with IPCs is one order of magnitude larger than that without IPCs, which suggested that the expected drop of conductivity caused by crosslinking was well compensated by the introduction IPCs. The network structure of polymer matrix of electrolyte film has excellent mechanical properties. Also, the chain structure of networks has significant effect both on ionic conductivity and on mechanical properties of CNPEs. A maximum conductivity of $1.01 \times 10^{-4} \text{ S cm}^{-1}$ and a maximum tensile strength of 0.66 MPa were obtained, respectively at 30 °C. Cyclic voltammetry indicates that CNPE did not oxidize until 4.3 V versus Li/Li⁺. As solvent free dry electrolytes, they exhibit good interfacial stability with electrode as indicated by ac impedance measurements using a symmetric cell, Li/CNPE/Li.

Acknowledgement

The authors gratefully acknowledge the financial support of the National Natural Science Foundation of PR China (Project No. 20333040).

References

- [1] D.E. Fenton, J.M. Parker, P.V. Wright, *Polymer* 14 (1973) 589.
- [2] F. Croce, G.B. Appetecchi, L. Persi, B. Scrosati, *Nature* 394 (1988) 456.
- [3] P. Lightfoot, M.A. Metha, P.G. Bruce, *Science* 262 (1993) 883.
- [4] J.M. Breen, H.S. Lee, X.Q. Yang, X. Sun, *J. Power Sources* 89 (2000) 163.
- [5] J.M. Song, H.R. Kang, S.W. Kim, W.M. Lee, H.T. Kim, *Electrochim. Acta* 48 (2003) 149.
- [6] M.K. Song, J.Y. Cho, B.W. Rhee, *J. Power Sources* 110 (2002) 209.
- [7] Z.C. Zhang, S.B. Fang, *J. Appl. Polym. Sci.* 77 (2000) 2957.
- [8] U.V. Alpen, A. Rabenau, G.H. Talat, *Appl. Phys. Lett.* 30 (1977) 621.
- [9] J. Cho, M. Liu, *Electrochim. Acta* 42 (1997) 1481.
- [10] M.K. Wang, L. Qi, F. Zhao, S.J. Dong, *J. Power Sources* 139 (2005) 224.
- [11] F. Croce, R. Curini, A. Martinelli, L. Persi, F. Ronci, B. Scrosati, R.J. Caminiti, *J. Phys. Chem. B* 103 (1999) 10632.
- [12] C. Capiglia, P. Mustarelli, E. Quartarone, C. Tomasi, A. Magistris, *Solid State Ionics* 118 (1999) 73.
- [13] C.S. Liao, W.B. Ye, *Electrochim. Acta* 49 (2004) 4993.
- [14] B. Kumar, L. Scanlon, R. Marsh, R. Higgins, R. Baldwin, *Electrochim. Acta* 46 (2001) 1515.
- [15] W.H. Hou, C.Y. Chen, C.C. Wang, *Solid State Ionics* 166 (2004) 399.
- [16] Z.C. Zhang, S.B. Fang, *Electrochim. Acta* 45 (2000) 2132.
- [17] Y.P. Wu, C. Wan, C. Jiang, S.B. Fang, *Lithium Ion Secondary Batteries*, Chemical Industry Press, Beijing, 2002, pp. 213.
- [18] Z.C. Zhang, J.J. Jin, F. Bautista, L.J. Lyons, N. Shariatzadeh, D. Sherlock, *Solid State Ionics* 170 (2004) 233.
- [19] H. Vogel, *Phys. Z.* 22 (1921).
- [20] V. Tamman, W. Hesse, *Allg. Chem.* 156 (1926) 245.
- [21] G. Fulcher, *J. Am. Chem. Soc.* 8 (1925) 339.
- [22] Y. Okamoto, T.F. Landel, H.S. Lee, T.A. Skotheim, *J. Polym. Soc., Part A: Polym. Chem.* 31 (1993) 2573.
- [23] X.J. Wang, J.J. Kang, Y.P. Wu, S.B. Fang, *Electrochem. Commun.* 5 (2003) 1028.
- [24] X.G. Yu, J.Y. Xie, J. Yang, K. Wang, *J. Power Sources* 132 (2004) 183.
- [25] W. Xu, X.G. Sun, C.A. Angel, *Electrochim. Acta* 48 (2003) 2256.
- [26] W.L. Qiu, X.H. Ma, Q.H. Yang, Y.B. Fu, X.F. Zong, *J. Power Sources* 138 (2004) 251.
- [27] Q. Li, T. Itoh, N. Imanishi, A. Hirano, Y. Takeda, O. Yamamoto, *Solid State Ionics* 159 (2003) 104.